ORIGINAL ARTICLE

Estimation and Compensation of the LuGre Friction Model in High-Speed Micro-Motion Control

Cong-Sheng Huang[1], Syh-Shiuh Yeh[2,*], and Pau-Lo Hsu[3]

[1]*Department of Electrical and Computer Engineering, North Carolina State University, NC, USA*

[2]*Department of Mechanical Engineering, National Taipei University of Technology, Taipei, Taiwan*

[3]*Department of Electrical Engineering, National Chiao Tung University, Hsinchu, Taiwan*

(**Received** 5 May 2017; **Accepted** 26 June 2017; **Published on line** 1 September 2017)

*Corresponding author: ssyeh@ntut.edu.tw

DOI: 10.5875/ausmt.v7i3.1400

Abstract: Static friction compensation is usually required to reduce friction in precision motion control and manufacturing processes. Micro-motion control is a current trend for precision machining in the electronics industry. Dynamic friction plays an important role in systems using micro-scale motion at high-speed and high-frequency command. The Lund–Grenoble (LuGre) friction model is suitable for coping with the dynamic friction effect. However, the parameters of this model are difficult to accurately identify to ensure satisfactory control performance in miniature machining. This paper proposes an efficient and systematic three-step parameter estimation method for LuGre modeling. The friction compensation of the proposed approach was successfully demonstrated on a 400W AC servo motor. Furthermore, under a peck drilling command on DYNA 1007 CNC machine, the LuGre model also improved motion precision by 72.0% in the maximum peak error.

Keywords: LuGre model, friction compensation, micro-motion, parameter estimation, peck drilling

Introduction

Precision motion control has emerged as a prominent issue in the development of light and slim commercial electronics. Peck drilling was originally applied for deep-hole drilling in geological research, oil exploration, or climate research. Special peck drilling applications for hard or fragile materials can effectively avoid tool and material damage during the drilling process. In recent years, peck drilling has also been widely adopted in the manufacturing of printed circuit boards (PCB) for cell phones, featuring strict requirements of limited size.

In deep-hole drilling applications with high-speed micro-motion control, friction is the most significant challenge during the drilling process. Friction is a nonlinear phenomenon and hence is difficult to address using traditional PID controllers, especially when the system is operating in micro motion at high speed with high-frequency commands [1]. In the past few decades, several nonlinear friction models have been proposed, including the Dahl model [2], the LuGre model [3-5], the Karnopp model [6], and the generalized Maxwell slip (GMS) [1, 7, 8]. In the CNC circular motion test, both quadrant glitches and stick-slip phenomena can be reduced by applying the nonlinear friction compensator (NFC) for static friction [9]. However, materials used for 3C industries have become even more rigid with a high-speed back-and-forth micro motion for PCB in peck drilling. Previous experimental results have shown that NFC is unsuitable for high-speed and high-frequency drilling commands under repetitive motion operations. The LuGre model [3-5], which is an extension from the Dahl model [2], captures the spring behavior and Stribeck effect. This model will be adopted in this study to investigate PCB peck drilling. In addition, different friction compensation approaches have been proposed such as observers [10-14], the extended Kalman filter [15, 16], neural networks [17, 18], and other approaches [19-22]. This paper adopts the feed-forward structure because of ease of use in industrial applications. Moreover, the LuGre model was combined with a feed-forward control, namely the inverse compensation filter [23, 24], to further improve motion accuracy [25].

NFC and the LuGre model were compared by increasing the magnitude of the sinusoidal wave. Experimental results indicate that friction force resulted in a significant degradation of micro-motion control performance. By applying the proposed LuGre-based friction compensation, motion precision is improved significantly compared with the use of traditional controllers.

Experimental Facility

Servo Motor

The experimental device consists of a digital signal processor (DSP)-based motion control board with a Delta 400W permanent magnet synchronous motor, as shown in Fig. 1. The servo motor specifications are listed in Table 1. The DSP-based motion control board with TI DSP TMS320F28335 includes the current feedback, speed, and position feedback loops. The current loop sampling frequency is 15 kHz, the speed loop sampling frequency is 7.5 kHz, and the position loop sampling frequency is 3.75 kHz.

CNC Machine

Peck drilling motion control was also conducted on the Z-axis of the DYNA MATE 1007 CNC machine, as shown in Fig. 2, with a 400 W servo motor similar to that specified in Table 1. The specifications of the CNC machine are listed in Table 2.

Cong-Sheng Huang received the B.S. degree in electrical engineering from the National Chung Hsing University, Taichung, Taiwan, in 2010, and the M.S. degree in electrical and control engineering from the National Chiao Tung University, Hsinchu, Taiwan, in 2012. He is currently a Ph.D. student in the department of electrical and computer engineering in the North Carolina State University, Raleigh, NC, USA. His research interests include system modeling, system monitoring, motor precision control.
Email: chuang15@ncsu.edu

Syh-Shiuh Yeh received the B.S. degree in mechanical engineering, the M.S. and Ph.D. degrees in electrical and control engineering from National Chiao Tung University, Taiwan, R.O.C., in 1994, 1996, and 2000, respectively. He was a researcher at the Mechanical Industry Research Laboratory, Industrial Technology Research Institute, R.O.C. He is currently an associate professor at the department of mechanical engineering, National Taipei University of Technology, R.O.C. His research interests include CNC Machine Tool Motion Control, Robotics and Manipulator Control, Dynamic Systems and Control. He is a member of IEEE, Chinese Automatic Control Society (CACS), and the Chinese Society of Mechanical Engineers (CSME).
Email: ssyeh@ntut.edu.tw

Pau-Lo Hsu (M'91) received the B.S. degree from National Cheng Kung University, Taiwan, the M.S. degree from the University of Delaware, and the Ph.D. degree from the University of Wisconsin-Madison, in 1978, 1984, and 1987, respectively, all in mechanical engineering. Following two years of military service in King-Men, he was with San-Yang (Honda) Industry during 1980-1981 and Sandvik (Taiwan) during 1981-1982. In 1988, he joined the Department of Electrical and Control Engineering, national Chiao Tung University, Hsinchu, Taiwan, R.O.C., as an Associate Professor. He became a Professor since 1995. During 1998-2000, he served as the Chairman of the department. He was elected as the President of the Chinese Automatic Control Society in 2001-2002. His research interests include mechantronics, CNC motion control, servo systems, and network control systems.
Email: plhsu@mail.nctu.edu.tw

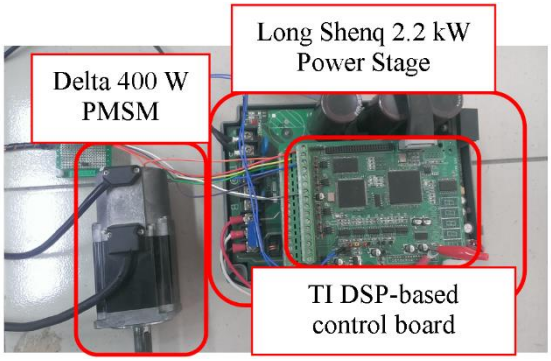

Figure 1. Experimental setup for the servo motor.

Table 1. Specifications of the Delta 400 Walt PMSM.

Rated power (kW)	0.4
Rated torque (N-m)	1.27
Maximum torque (N-m)	3.82
Rated angular velocity (rpm)	3,000
Maximum angular velocity (rpm)	5,000
Rotor inertia (kg-m^2)	0.34×10^{-4}
Encoder resolution (encoder increments/ revolution)	10,000
Encoder resolution (radian/encoder increment)	6.2832×10^{-4}

Figure 2. DYNA MYTE 1007 CNC machine.

Table 2. CNC machine specifications.

X table travel (mm)	250
Y table travel (mm)	175
Z table travel (mm)	250
Z-axis Position precision (mm)	0.001

Static NFC Friction Modeling

With the static friction model, the NFC is adopted directly in the CNC to compensate for the friction effect with relatively low frequency commands. The NFC is

applied effectively to a circular contouring motion to cope with quadrant glitches and stick-slip. Ideally, the electrical current flowing into the motor should be zero if the motor is operated at a constant speed. In practice, friction and disturbance will require extra torque to maintain the desired constant speed. Therefore, the difference between the actual measured current $i_{q,act}$, which flows into the motor driver, and the current $i_{q,ref}$, which is generated by power stage, can be expressed as follows:

$$i_{q,act} = i_{q,ref} - i_{friction} - i_{disturbane} \quad (1)$$

where $i_{disturbance}$ is the disturbance and $i_{friction}$ is the sum of all friction effects. If the motor is operated in a disturbance-free situation, then the corresponding mechanical equation can be expressed simply as follows:

$$J\frac{d\omega_m}{dt} = K_t i_{q,act} = K_t(i_{q,ref} - i_{friction}) \quad (2)$$

At a constant-speed motion, Eq. (2) becomes zero and $i_{q,ref}$ equals to $i_{friction}$. Thus, the static friction model can be constructed with different constant speed commands ω_{ref}, and the obtained static friction model can be adopted as a feed-forward compensator to achieve static NFC friction compensation [9], as shown in Fig. 3. Note that K_n is an adjustable percentage gain with practical implications in real applications.

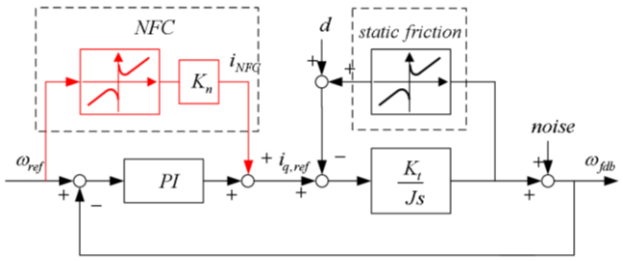

Figure 3. Control structure of applying the static NFC friction compensator.

Figure 4 shows that, by applying the least-square approach for the measured friction, the static nonlinear friction model in polynomial functions can be obtained as follows:

$$i_{NFC} = \begin{cases} 0.00000031\omega^2 - 0.00007343\omega + 0.02586770 \\ \quad 0 \le \omega < 70\,\text{rpm} \\ 0.00001756\omega + 0.02089632 \\ \quad 70 \le \omega < 3000\,\text{rpm} \\ -0.00000041\omega^2 - 0.00009596\omega - 0.0269025 \\ \quad 0 \ge \omega > -70\,\text{rpm} \\ 0.00001539\omega - 0.02124245 \\ \quad -70 \ge \omega > -3000\,\text{rpm} \end{cases} \quad (3)$$

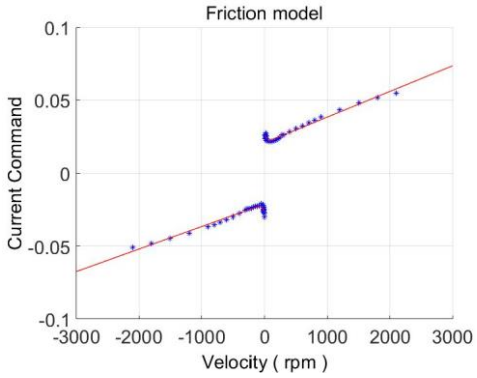

Figure 4. Identified static nonlinear friction curve.

As shown in Fig. 5, a sinusoidal-like wave with increasing magnitude is an approximated command for performing PCB peck drilling. The control tracking error with P controller at the initial stage is significant, as shown in Fig. 6. As shown in Fig. 3, applying the NFC improves system response. However, the system performance at each turning point was still poor because NFC friction compensation was fed directly to the motion system without further processing its dynamic friction effect. Therefore, applying the static NFC compensator is unsuitable for PCB peck drilling, and either the material or drill may be easily damaged because of its rough motion.

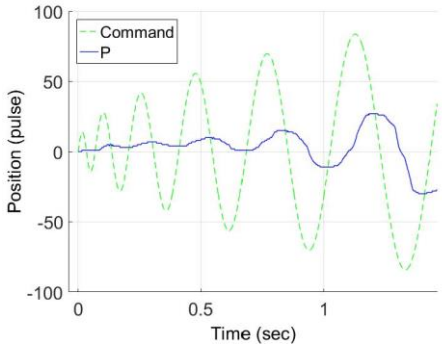

Figure 5. Servo motor response applying the P controller.

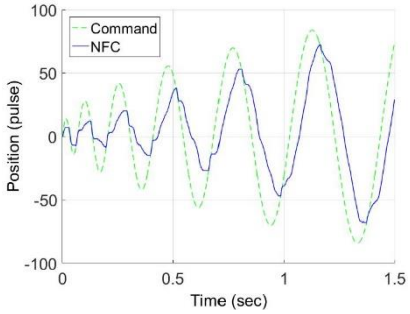

Figure 6. Servo motor response applying the P controller with NFC.

LuGre Friction Modeling on Motors

LuGre Model Structure

The LuGre friction model was originally proposed in

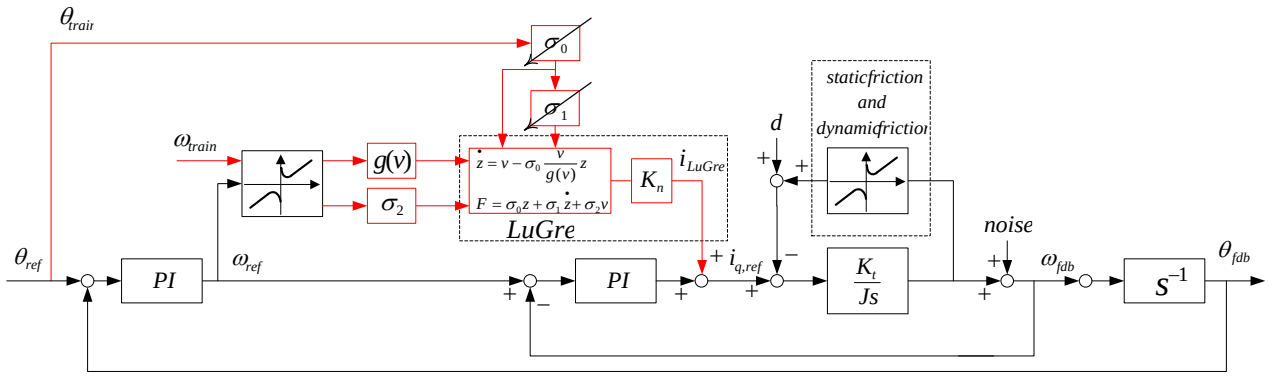

Figure 7. Illustration of the three-step parameter estimation approach of the LuGre model.

1995 [3]. An extension of the Dahl model, the LuGre model captures two additional friction characteristics, namely the Stribeck effect and stick-slip motion. In 2008, the LuGre model was further modified as follows [5]:

$$\dot{z} = v - \sigma_0 \frac{v}{g(v)} z = v - h(v) z \,, \tag{4}$$

$$F(z, v) = \sigma_0 z + \sigma_1 \dot{z} + f(v) \,, \tag{5}$$

where

$$g(v) = F_c + (F_s - F_c) e^{-|v/v_s|^{\alpha}} \,, \tag{6}$$

$$f(v) = \sigma_2 v \,. \tag{7}$$

The static part of the LuGre friction model can be obtained while the system is operating under a constant speed as follows:

$$F_{ss}(v) = \sigma_0 z + f(v) = g(v)\,\mathrm{sgn}(v) + f(v) \,, \tag{8}$$

where σ_0 refers to stiffness, σ_1 indicates micro-damping, σ_2 is a parameter for viscous friction, z is the state of friction, F_c is Coulomb friction, F_s is static friction, v is the velocity between two surfaces, and v_s is the Stribeck velocity. Bristles deform when two surfaces in contact move against each other, and the deformation can be recognized as a friction force. State z indicates this bristle deformation in the LuGre model. $F(v) = \sigma_2 v$ means viscous friction, which is related to velocity. $g(v)$ is a positive function to describe the Stribeck effect. The value of α is controversial; some researchers claim that $\alpha = 1$ [3, 11, 13], whereas others claim that $\alpha = 2$ [12, 19]. In the present approach, α would not be obtained and a static friction model will be adopted directly from NFC to determine $g(v)$ and σ_2.

The most crucial parameter σ_1 in micro-scale position precision control represents damping in the pre-sliding displacement. A three-step method is proposed to identify the three parameters of the LuGre model, as shown in Fig. 7. An adjustable percentage gain K_n is also preferred for real concerns in applications. The K_n is the proportional gain in the feedforward friction compensation. The friction compensation algorithm should help the system overcome static friction, but it cannot apply excessive force after the motor starts moving; otherwise, the system will oscillate to suppress the additional force generated by the algorithm. The LuGre model can capture this changing state, hence the nominal value of K_n should be set as 1. However, the value of K_n should be slightly less than 1 since the current closed-loop control in the motor control system also contributes to error reduction. In the paper, the K_n is set as 0.8.

Determination of LuGre Model Parameters

This paper proposes a three-step, systematic parameter estimation method by following the physical meaning of each variable. Thus the number of identified parameters is reduced to three. In the first step, the dynamic part of the LuGre model is isolated at a constant speed such that σ_2 is obtained and $g(v)$ is also determined, as shown in Fig. 8. State $\dot{z}$ in the model will approach zero at static operation, and $\sigma_1 \dot{z}$ has no effect on static friction identification when the system reaches a steady state. Parameters $g(v)$ and σ_2 p
resent the static part of the Stribeck effect, which can be calculated from the static friction model through Eqs. (7) and (8).

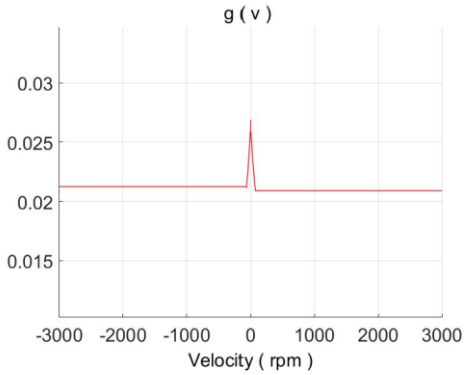

Figure 8. $g(v)$ of the Delta 400 W motor.

As the σ_2 is determined in the first step, σ_0 and σ_1 remain to be identified. σ_0 has almost no effect on the force profile, but yields a larger force peak by selecting a smaller value [26]. A larger σ_0 will also lead to better stability, and σ_0 has a boundary similar to that in [5]. Experiments show that the motor will generate unexpected noise as σ_0 gradually increases until it exceeds the boundary. Hence, a systematic adjusting procedure to obtain all parameters in the LuGre model is described in Fig. 7. In the final step, σ_1 is tuned to obtain the minimal RMS.

Tuning the three parameters for the LuGre model can be summarized as a three-step approach as follows:

Step_1. Calculate σ_2 and $g(v)$ from the static friction model between the velocity of the static friction model and the slope of viscous friction.

Step_2. Set σ_1=0, tune σ_0 with a sinusoidal wave (for example, $400\sin(8\pi \cdot t)$) or a ramp command. Increase σ_0 from a very small non-zero value until the tracking error is reduced to a certain level, as shown in Fig. 9. For example, σ_0 is selected as 0.040.

Step_3. Tune σ_1 by using the same sinusoidal wave or the same ramp command. Similar to step 2, increase σ_1 from a very small non-zero value until the RMS tracking error reduces to a preset value, as shown in Fig. 10. A small σ_1 cannot provide enough force to overcome the friction force, as shown in Figs. 11 and 14. However, too large a σ_1 will also result in a peak when the system starts moving thus, as shown in Figs. 11 and 14, σ_1=0.017 was properly chosen in this paper.

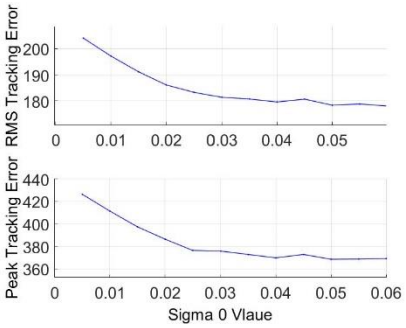

Figure 9. RMS error with different σ_0 (sinusoidal command).

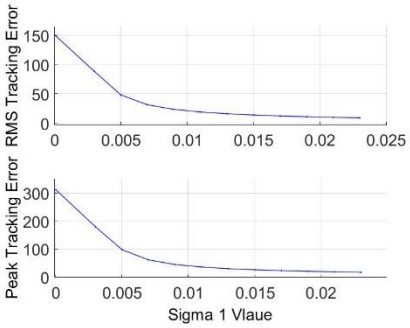

Figure 10. RMS error with different σ_1 (sinusoidal command).

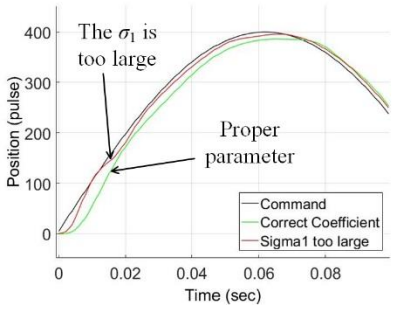

Figure 11. System response with large σ_1 (sinusoidal command).

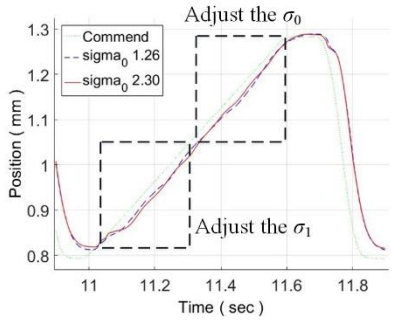

Figure 12. System responses with tuned σ_0 and σ_1 (ramp command).

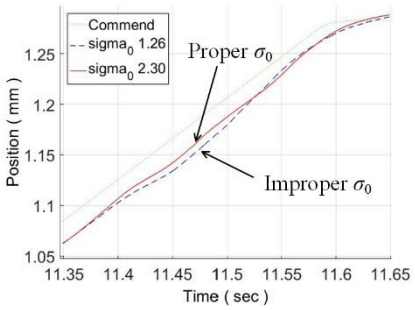

Figure 13. System responses with tuned σ_0 (ramp command).

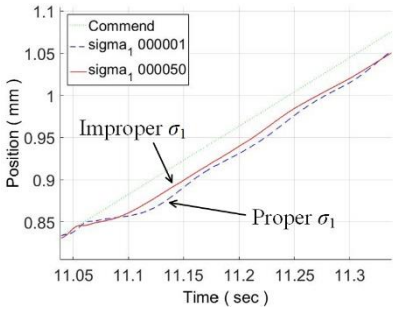

Figure 14. System responses with tuned σ_1 (ramp command).

The obtained corresponding parameters are shown in Table 3. As shown in Fig. 15, satisfactory performance was obtained by applying the LuGre model for friction compensation. The system moved perfectly by following the motion command, even at the first wave. In addition, the motor system moved smoothly by including the LuGre compensation. Thus, this result also shows the usefulness of the LuGre friction model and proves the feasibility of the three-step LuGre model parameter estimation method. In this study, the parameters of the applied PI

velocity feedback controller were manually tuned to achieve rapid velocity responses of the servo axis. The parameters of the applied PI position feedback controller were also manually tuned to achieve rapid position responses of the servo axis. After tuning the PI control parameters, the proposed estimation and compensation approaches based on the LuGre friction model were applied to the PI-controlled servo axes to further improve reversal responses during the period of axial motion.

Table 3. LuGre model parameters for the motor

Coeff.	Clockwise	Anti-clockwise
σ_0	0.040	
σ_1	0.017	
σ_2	1.756×10^{-5}	1.539×10^{-5}
F_c	0.0209	0.0212
F_s	0.0259	0.0269

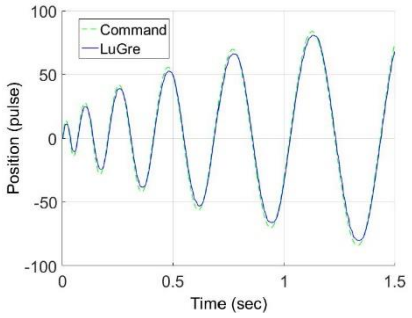

Figure 15. Servo motor response with the LuGre model.

Experimental Results on the CNC

The CNC machine with a perpendicular Z-axis moving table causes more significant friction effect than the servo motor alone. Figure 16 shows that the CNC machine Z-axis barely moves when operated under peck drilling command, even with well-tuned PI controllers for both current and speed loops, and the position loop with the P controller. The static friction model was obtained with the measured friction force under different constant speeds as shown in Fig. 17. Figure 18 shows that the CNC Z-axis moved with improved performance after NFC friction compensation was applied.

Finally, the LuGre model was applied to CNC machines, and the function $g(v)$ as shown in Fig. 19 was obtained from Fig. 17. The parameters of the LuGre model obtained from the proposed three-step approach were applied to the CNC machine, as listed in Table 4. The CNC system followed the drilling command successfully after applying the LuGre model friction compensation, even at the initial stage with relatively low-frequency command, as shown in Fig. 20.

The peck drilling results on CNC machine with different friction compensators are summarized in Tables 5 and 6. The experimental results indicate that applying the LuGre model, the tracking error in the RMS value is significantly improved (67.5%) in the direction of engaged motion. The maximum error also presents an obvious improvement of 72%.

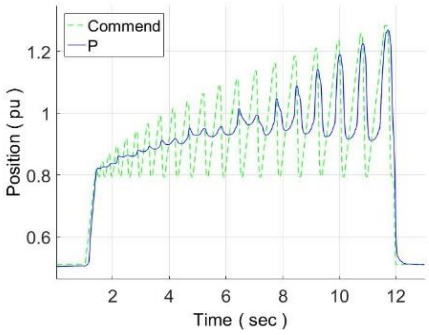

Figure 16. CNC response with the P controller.

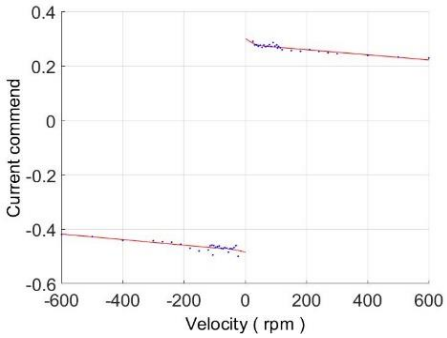

Figure 17. Static friction model of Z-axis of CNC.

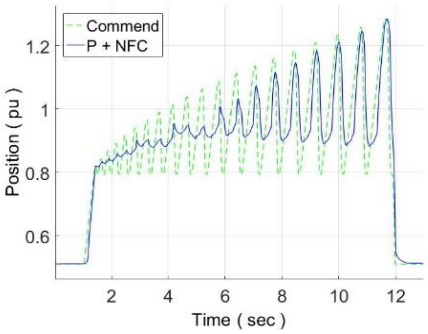

Figure 18. CNC response with NFC friction compensation.

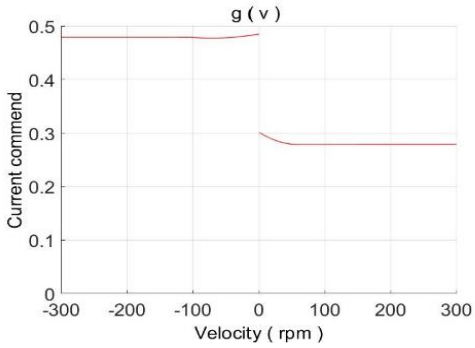

Figure 19. Function $g(v)$ of CNC.

Table 4. Parameters of Z-axis of the CNC machine

Coeff.	Value	
	Clockwise	Anti-clockwise
σ_0	2.3	
σ_1	7.3x10^{-5}	
σ_2	-9.410x10^{-6}	-1.018x10^{-5}
F_c	0.286	0.480
F_s	0.301	0.485

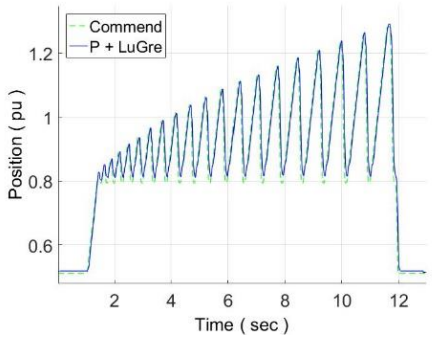

Figure 20. CNC response with the LuGre model.

Table 5. Tracking error RMS with the LuGre model

Controller	Engage		Retract	
	Tracking error Avg. (um)	Improve ratio Avg. (%)	Tracking error Avg.(um)	Improve ratio Avg. (%)
P	90.112	-	75.937	-
P+NFC	79.974	11.2	70.386	1.7
P+LuGre	24.150	67.5	30.003	41.0

Table 6. Maximum tracking error with the LuGre model

Controller	Engage		Retract	
	Tracking error Avg. (um)	Improve ratio Avg. (%)	Tracking error Avg. (um)	Improve ratio Avg. (%)
P	133.466	-	167.522	-
P+NFC	118.413	11.8	173.073	-3.3
P+LuGre	25.064	72.0	13.097	34.7

Conclusion

The proposed three-step parameter identification approach uses the static NFC as the basic friction model and is incorporated into the dynamic LuGre friction model. In the first step, two parameters, namely, σ_2 and $g(v)$, can be easily obtained from the static friction force which equals to $g(v)+\sigma_2 v$. The dynamic LuGre friction model is then obtained. Considering that the parameters of the LuGre model are difficult to obtain properly, the tracking error RMS value of the time response can be used to adjust σ_0 and σ_1. σ_1 directly influences the system response at motion turning points. Therefore, the present three-step approach will first tune σ_0, and then tune the parameter σ_1. As σ_0 increases, the tracking error in the RMS value is reduced. A relatively small σ_0 is preferred without affecting the final friction compensation. Once σ_0 is selected, σ_1 is identified and is tuned until the time response meets requirements.

In contrast with NFC, the LuGre model can respond flexibly to various conditions by tuning σ_0 and σ_1. Here, σ_0 and σ_1 remain unchanged (σ_0 =0.040 and σ_1 =0.017) even with different amplitudes and input frequencies of the sinusoidal commands. However, the optimal σ_0 and σ_1 values vary (σ_0 =0.018 and σ_1 =0.018) as peck drilling commands are applied. Furthermore, σ_0 and σ_1 also change in the peck drilling motion on the CNC machine (σ_0 =2.3 and σ_1 = 7.3×10^{-5}). Hence, experimental results indicate that σ_0 and σ_1 should be tuned case by case to obtain best performance in real applications.

A simple approach of estimating the LuGre friction model parameters with three steps is proposed. The LuGre model using this parameter estimation approach was applied successfully to both the AC servo motor and the CNC machine with significantly improved motion precision even under high-speed micro-motion operations, usually adopted in PCB peck drilling. With the proposed parameter estimation method for LuGre modeling, the most suitable model parameters with different commands can be obtained on a case by case basis. PCB peck drilling on CNC machines is a novel technique, particularly for hard or fragile materials. By applying the proposed LuGre-based friction compensation, the performance of both the servo motor and the CNC machine can be significantly improved. One of the contributions of this paper is to reduce the application complexity of the LuGre friction model by finding the three most significant variables in the model and then testing their performance. This can facilitate industrial adoption.

Acknowledgment

This project was supported in part by the Ministry of Science and Technology, Taiwan, under Contract MOST104-2221-E-027-132 and MOST103-2218-E-009-027-MY2.

References

[1] Y.-F. Liu, J. Li, Z.-M. Zhang, X.-H. Hu, and W.-J. Zhang, "Experimental comparison of five friction models on the same test-bed of the micro stick-slip motion system," *Mechanical Sciences*, vol. 6, no. 1, pp. 15-28, March 2015.
doi: 10.5194/ms-6-15-2015

[2] P. Dahl, "A solid friction model," Aerospace Corp., Los Angeles, CA, USA, Tech. Rpe. TOR-0158(3107–18)-1, 1968.

[3] C. Canudas-de-Wit, H. Olsson, K. J. Astrom, and P. Lischinsky, "A new model for control of systems with friction," *IEEE Transactions on Automatic Control*, vol. 40, no. 3, pp. 419-425, March 1995.
doi: 10.1109/9.376053

[4] Y.-H. Sun, Y. Sun, C. Q. Wu, and N. Sepehri, "Stability analysis of a controlled mechanical system with parametric uncertainties in LuGre friction model," *International Journal of Control*, pp. 1-14, Feb. 2017.
doi: 10.1080/00207179.2017.1293846

[5] K. J. Astrom and C. Canudas-de-Wit, "Revisiting the LuGre friction model," *IEEE Control Systems Magazine*, vol. 28, no. 6, pp. 101-114, Nov. 2008.
doi: 10.1109/MCS.2008.929425

[6] D. Karnopp, "Computer simulation of stick-slip friction in mechanical dynamic systems," *Journal of Dynamic Systems, Measurement and Control, Transactions of the ASME*, vol. 107, no. 1, pp. 100-103, July 1985.
doi: 10.1115/1.3140698

[7] F. Al-Bender, V. Lampaert, and J. Swevers, "The generalized Maxwell-slip model: A novel model for friction simulation and compensation," *IEEE Transactions on Automatic Control*, vol. 50, no. 11, pp. 1883-1887, Nov. 2005.
doi: 10.1109/TAC.2005.858676

[8] M. Boegli, T. De Laet, J. De Schutter, and J. Swevers, "A smoothed GMS friction model suited for gradient-based friction state and parameter estimation," *IEEE/ASME Transactions on Mechatronics*, vol. 19, no. 5, pp. 1593-1602, Oct. 2014.
doi:10.1109/TMECH.2013.2288944

[9] W.-S. Huang, C.-W. Liu, P.-L. Hsu, and S.-S. Yeh, "Precision control and compensation of servomotors and machine tools via the disturbance observer," *IEEE Transactions on Industrial Electronics*, vol. 57, no. 1, pp. 420-429, Jan. 2010.
doi: 10.1109/TIE.2009.2034178

[10] W. Lee, C.-Y. Lee, Y.-H. Jeong, and B.-K. Min, "Distributed Component Friction Model for Precision Control of a Feed Drive System," *IEEE/ASME Transactions on Mechatronics*, vol. 20, no. 4, pp. 1966-1974, Aug. 2015.
doi: 10.1109/TMECH.2014.2365958

[11] J. Ishikawa, S. Tei, D. Hoshino, M. Izutsu, and N. Kamamichi, "Friction compensation based on the LuGre friction model," in proceeding of *the SICE Annual Conference*, Taipei, Taiwan, Aug. 18-21, 2010, pp. 9-12.

[12] T. H. Lee, K. K. Tan, and S. Huang, "Adaptive friction compensation with a dynamical friction model," *IEEE/ASME Transactions on Mechatronics*, vol. 16, no. 1, pp. 133-140, Feb. 2011.
doi: 10.1109/TMECH.2009.2036994

[13] D. Hoshino, N. Kamamichi, and J. Ishikawa, "Friction compensation using time variant disturbance observer based on the LuGre model," in proceeding of *the 12th IEEE International Workshop on Advanced Motion Control*, Sarajeco, Bosnia-Herzegovina, March 25-27, 2012.
doi: 10.1109/AMC.2012.6197030

[14] M. Ruderman and M. Iwasaki, "Observer of nonlinear friction dynamics for motion control," *IEEE Transactions on Industrial Electronics*, vol. 62, no. 9, pp. 5941-5949, Sept. 2015.
doi: 10.1109/TIE.2015.2435002

[15] B. J. E. Misgeld, M. Kramer, and S. Leonhardt, "Multivariable friction compensation control for a variable stiffness actuator," *Control Engineering Practice*, vol. 58, pp. 298-306, Jan. 2017.
doi: 10.1016/j.conengprac.2015.08.013

[16] L. Lu, B. Yao, Q. Wang, and Z. Chen, "Adaptive robust control of linear motor systems with dynamic friction compensation using modified LuGre model," in proceeding of *the 2008 IEEE/ASME International Conference on Advanced Intelligent Mechatronics*, Xian, China, July 2-5, 2008, pp. 961-966.
doi: 10.1109/AIM.2008.4601791

[17] H. Donath, S. Georg, and H. Schulte, "Takagi-Sugeno sliding mode observer for friction compensation with application to an inverted pendulum," in proceeding of *the IEEE International Conference on Fuzzy Systems*, Hyderabad, India, July 7-10, 2013.
doi: 10.1109/FUZZ-IEEE.2013.6622558

[18] J. Yao, Z. Jiao, and D. Ma, "RISE-based precision motion control of DC motors with continuous friction compensation," *IEEE Transactions on Industrial Electronics*, vol. 61, no. 12, pp. 7067-7075, May 2014.
doi: 10.1109/TIE.2014.2321344

[19] H. Chaoui and P. Sicard, "Adaptive fuzzy logic control of permanent magnet synchronous machines with nonlinear friction," *IEEE Transactions on Industrial Electronics*, vol. 59, no. 2, pp. 1123-1133, Feb. 2012.
doi: 10.1109/TIE.2011.2148678

[20] M. Tomizuka, "Zero phase error tracking algorithm for digital control," *Journal of Dynamic Systems, Measurement and Control,* vol. 190, no. 1, pp. 65-68, Mar. 1987.
doi: 10.1115/1.3143822

[21] M. Weck and G. Ye, "Sharp corner tracking using the IKF control strategy," *CIRP Annals - Manufacturing Technology*, vol. 39, no. 1, pp. 437-441, 1990.
doi:10.1016/S0007-8506(07)61091-9

[22] C.-S. Huang, S.-S. Yeh, and P.-L. Hsu, "Design the high-speed micro-motion controller for peck drilling with the LuGre friction model," in proceeding of *the ASME International Mechanical Engineering Congress and Exposition*, Montreal, Canada, Nov. 14-20, 2014.
doi:10.1115/IMECE2014-36152

[23] A. Asadian, M. R. Kermani, and R. V. Patel, "A novel force modeling scheme for needle insertion using multiple Kalman filters," *IEEE Transactions on Instrumentation and Measurement*, vol. 61, no. 2, pp. 429-438, Feb. 2012.
doi:10.1109/TIM.2011.2169178